



## Wall-to-bed mass transfer in three-phase fluidized beds in the absence and presence of a composite promoter

K.V. Ramesh<sup>a,\*</sup>, G.M.J. Raju<sup>a</sup>, M.S.N. Murty<sup>b</sup>, C. Bhaskara Sarma<sup>b</sup>

<sup>a</sup> Department of Chemical Engineering, Andhra University, Visakhapatnam 530003, India

<sup>b</sup> Department of Chemical Engineering, GVP College of Engineering, Visakhapatnam 530048, India

### ARTICLE INFO

#### Article history:

Received 24 January 2008

Received in revised form 3 April 2009

Accepted 16 April 2009

#### Keywords:

Three-phase fluidization  
Gas–liquid fluidization  
Wall-to-bed mass transfer  
Turbulent promoter

### ABSTRACT

Wall-to-bed mass transfer coefficients were computed in a three-phase fluidized bed in plain annuli and in the absence and presence of a helicoidal tape wound on a coaxial central rod of varying diameters using electrochemical technique. Glass spheres were used as solid phase, an electrolyte (equimolar ferri–ferrocyanide solution) as liquid-phase and nitrogen as gaseous phase. The test section was an acrylic cylindrical column of 6.73 cm i.d. Limiting current measurements were made at point copper electrodes fixed flush with the test section, which facilitated the computation of wall-to-bed mass transfer coefficients. Augmentation in wall-to-bed mass transfer coefficient was found to be significant with increased liquid and gas velocities, and particle diameter. The presence of composite promoter showed significant improvements in the wall-to-bed mass transfer coefficients. The data on wall-to-bed mass transfer coefficient were correlated in terms of Coulburn  $j_D$  factor, individual phase holdups, particle Reynolds number and geometrical parameters of the composite promoter as  $j_D \varepsilon_L = 0.14 [((Re_p \varepsilon) / (\varepsilon_L (1 - \varepsilon))) (1 + (p/D_c))]^{-0.23}$ .

© 2009 Elsevier B.V. All rights reserved.

### 1. Introduction

Gas–liquid–solid fluidized and packed beds are commonly used as three-phase contactors in various chemical processes. Three-phase fluidized beds find applications in chemical, petrochemical and bioprocessing industries, specific being those in catalytic hydrogenation and oxidation. The objective of the present study is to evaluate the mass transfer coefficients at the confining wall of an electrochemical reactor in the presence of a turbulence promoter element in a three-phase fluidized bed. The effect of geometric variables of the promoter are subsequently investigated and presented. A correlation has been developed to optimize various variables covered in the present study based on which the design and operation of the electrochemical reactor could be carried out.

The rate of wall-to-bed heat or mass transfer is an essential factor in the design and operation of such contacting equipment. It was observed that the wall-to-bed mass transfer rates could be significantly increased by introducing the gas-phase into a two-phase liquid–solid fluidized or packed bed because of agitation or turbulence promoted by the gas-phase. Very few studies [1–5] have been reported on wall-to-bed mass transfer in three-phase fluidized beds. It is well known that overall mass transfer rates can be augmented by the presence of turbulence promoters or circu-

lating solids of inert particles. Several investigations were found in literature on turbulence promoters used for augmentation of heat and mass transfer coefficients in homogeneous flow and in fluidized beds. Bergles [6] made an exhaustive review on evaluation of techniques of augmentation. However, investigations on the magnitudes of augmentation in three-phase fluidized beds in the presence of an insert promoter assembly are scarce.

Electrochemical processes demand high mass transfer rates at reduced surface areas; offer lower capital investment and achieve high production rates. In order to obtain high mass transfer rates in an electrochemical cell, one can either increase the driving force and/or augment the mass transfer coefficient. The former however could be achieved by reaching the limiting current condition in diffusion controlled electrode reactions. Conventionally, either turbulence promoters or the fluidizing bed of inert particles have been in practice to augment the overall heat and mass transfer rates between a flowing electrolyte and a wall.

The introduction of a gas into a liquid–solid fluidized bed was found to be advantageous as it enhances turbulence resulting in increased mass transfer as discussed elsewhere [2,3]. Further, when a helicoidal tape promoter is inserted in a three-phase fluidized bed, swirl flow may be visualized and the swirl generated due to the flow of the fluid past the boundaries of the helical tape element induces its radial component into the axial flow. As the axial flow is increased the radial component progressively moves towards the confining wall resulting in a tractive shear along the wall over which the transfer reactions

\* Corresponding author. Tel.: +91 9490109683; fax: +91 891 2537793.  
E-mail address: [kvramesh69@yahoo.com](mailto:kvramesh69@yahoo.com) (K.V. Ramesh).

### Nomenclature

$A$	surface area of electrode ( $\text{m}^2$ )
$C_0$	bulk concentration of the reactant ion ( $\text{kmol}/\text{m}^3$ )
$d_p$	diameter of the particle (m)
$d_r$	diameter of the rod (m)
$D_c$	diameter of the test section (m)
$D_e$	equivalent diameter (m)
$D_L$	diffusivity of reacting species ( $\text{m}^2/\text{s}$ )
$D_0$	obstruction diameter (m)
$F$	Faraday's constant (C)
$g$	acceleration due to gravity, $9.81 \text{ (m/s}^2\text{)}$
$H$	fluidized bed height (m)
$i_L$	limiting current (A)
$k_L$	liquid to wall mass transfer coefficient (m/s)
$p$	pitch of the tape (m)
$Q_g$	gas-flow rate ( $\text{m}^3/\text{s}$ )
$Q_L$	liquid-flow rate ( $\text{m}^3/\text{s}$ )
$t$	thickness of tape (m)
$U_g$	gas superficial velocity (m/s)
$U_L$	liquid superficial velocity (m/s)
$w$	tape width (m)
$W_s$	weight of solids in the bed (kg)
$z$	number of electrons per ion reacted at electrode surface

### Greek letters

$\varepsilon$	bed porosity
$\varepsilon_g$	gas holdup
$\varepsilon_L$	liquid holdup
$\varepsilon_s$	solids holdup
$\mu$	viscosity of electrolyte ( $\text{kg}/\text{m s}$ )
$\rho$	density of gas ( $\text{kg}/\text{m}^3$ )
$\rho_L$	liquid density ( $\text{kg}/\text{m}^3$ )
$\rho_s$	density of particles ( $\text{kg}/\text{m}^3$ )

### Dimensionless numbers

$j_D$	Coulburn $j$ -factor, $k_L Sc^{2/3}/U_L$
$Re_p$	Reynolds number based on particle diameter, $\rho_L d_p U_L/\mu$
$Sc$	Schmidt number, $\mu/\rho D_L$

(redox) are taking place. The turbulent mixing of the fluid elements is thus, expected to contribute higher augmentation in the wall mass transfer coefficients at the confining wall. Augmentation of the wall mass transfer coefficients can further be attributed to the effective reduction in the boundary layer thickness due to the prevailing tractive shear at the electrode surface. The combined effect of swirl flow superimposed on the complex phenomena of three-phase fluidization would also contribute towards the reduction in the boundary layer thickness considerably.

Interstitial velocity of the continuous liquid-phase is further increased due to the presence of gas-phase, leading to vigorous stirring of the bed. The fluidized bed condition might be expected to attain at a fluid velocity far lower than that found in liquid–solid systems due to the additional momentum induced by gaseous phase. In view of this, an attempt has been made to evaluate the effect of various pertinent dynamic and geometric variables on wall mass transfer coefficient for the reduction of ferricyanide ion in three-phase fluidized beds in plain annuli and also in the absence and presence of composite helicoidal tape promoter.

## 2. Experimental

The equipment was designed and fabricated to carryout studies on wall-to-bed mass transfer at the inner surface of the outer column of an electrochemical cell. Twisted tapes wound on a rod were used as composite promoter, which was placed concentrically in the electrochemical cell.

The schematic of the experimental set-up used in these studies was shown in Fig. 1. The equipment and apparatus consisted of a cylindrical storage tank (S), centrifugal pump (P) for circulating the electrolyte, two rotameters ( $R_1$  and  $R_2$ ) for measuring the flow rate of the electrolyte, a nitrogen cylinder (N) for supply of nitrogen gas, a wet gas meter (G) for metering the nitrogen gas, pressure regulators to regulate the nitrogen flow from the high pressure cylinder with two pressure gauges ( $P_1$  and  $P_2$ ).  $P_1$  indicates pressure inside the nitrogen cylinder, and  $P_2$  shows the reduced outlet pressure. Two open manometers ( $M_1$  and  $M_2$ ) were used:  $M_1$  to measure the pressure at the wet gas meter,  $M_2$  to measure the pressure in the test section. A U-tube differential manometer (U) was provided to measure the pressure difference across the test section (B). Valves  $V_1$  to  $V_6$  were used to control the flow rates of liquid while valves  $V_7$  to  $V_9$  were used to control the flow rate of the gas through the experimental column.

The test section (B), which served as a fluidizing column, was made of smooth Perspex tube of 6.73 cm inner diameter and 0.6 m height. The inner wall of the test section was provided with copper point electrodes of diameter 3.42 mm. The point electrodes 8 in number were machined to the size out of 4 mm diameter copper rod. One end of these electrodes was fixed flush with the surface of the inner wall of the test section while the other end projected outward served as terminal for connecting the electrodes to the external circuit. Two pressure taps ( $T_1$ ) at the bottom flange and ( $T_2$ ) at the top flange have been provided across the test section for pressure drop measurements. The taps ( $T_1$  and  $T_2$ ) were connected to the limbs of the U-tube manometer to measure the pressure drop. Carbon tetrachloride was used as manometric fluid. A stainless steel wire mesh (W) was placed at the bottom of the test section to support the bed of solids and allow uniform distribution of liquid and gas in the test section during fluidization experiments. The composite promoter element was essentially a copper or stainless steel rod of diameter  $d_r$ , on the outer surface of which, a tape of given width  $w$ , thickness  $t$  was wound and brazed helicoidally at a desired pitch  $p$ . Promoter elements of different geometrical characteristics (viz., diameter  $d_r$ , pitch  $p$ , width  $w$  and thickness  $t$ ) were used. Prior to the assembly of the test section, the surfaces of the point electrodes were polished with a three zero emery paper, cleaned thoroughly, degreased and activated.

The electrolyte from the storage tank was metered through rotameters ( $R_1$  and  $R_2$ ) and circulated through the test section. After the flow was stabilized, nitrogen gas metered through a wet-gas meter, was bubbled through a sparger provided at the bottom end of the entrance calming section. When the liquid- and gas-flow rates were stabilized, the limiting current was measured by applying an electric potential in small increments between the test electrode and the wall electrode.

The bed materials used in the present investigation were spherical glass balls of three different diameters, viz., 3.13, 4.57 and 6.39 mm. Mass transfer coefficients were evaluated from the measured limiting current data for various combinations of gas-flow rate  $Q_g$ , liquid-flow rate  $Q_L$ , bed porosity  $\varepsilon$ , pitch  $p$ , width  $w$  and diameter of the rod of the composite promoter element  $d_r$ . Eq. (1) is used to obtain wall-to-bed mass transfer coefficients, the derivation of which was given elsewhere [7]. Range of variables covered is presented in Table 1:

$$k_L = \frac{i_L}{zFAC_0} \quad (1)$$

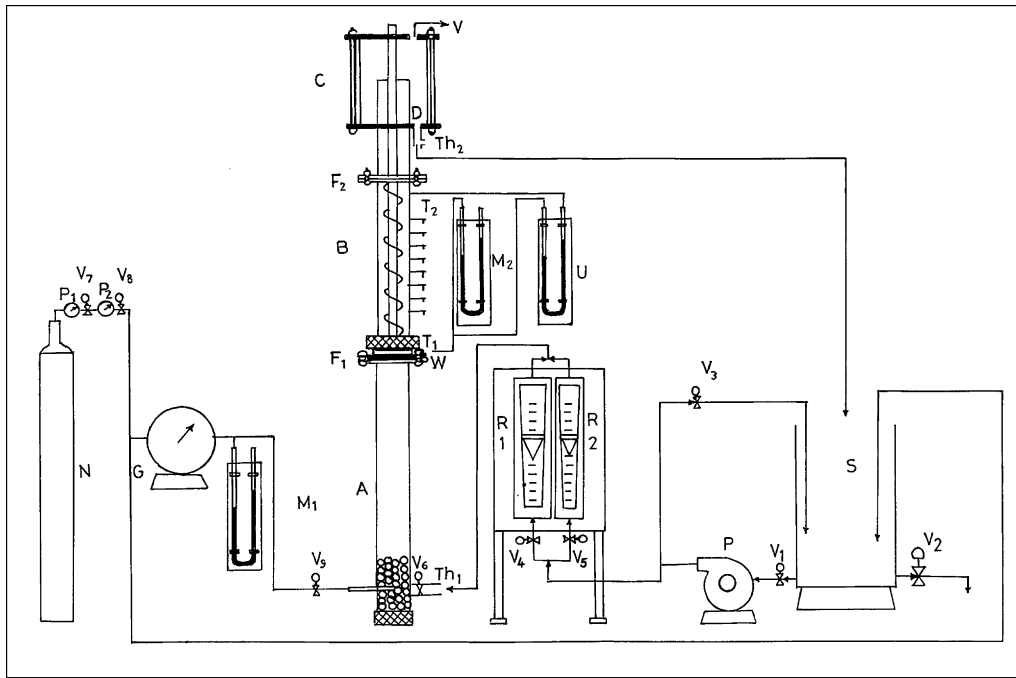


**Fig. 1.** Schematic of experimental unit. A, entrance calming section; B, test section; C, exit section; D, drain; F<sub>1</sub> and F<sub>2</sub>, flanges; G, wet gas meter; M<sub>1</sub> and M<sub>2</sub>, open end manometers; N, nitrogen gas cylinder; P, pump; P<sub>1</sub> and P<sub>2</sub>, pressure gages; R<sub>1</sub> and R<sub>2</sub>, rotameters; S, storage tank; T<sub>1</sub> and T<sub>2</sub>, pressure taps; Th<sub>1</sub> and Th<sub>2</sub>, thermocouples, U, U-tube manometer; V, vent; V<sub>1</sub> to V<sub>9</sub>, valves; W, wire mesh.

The wall-to-bed mass transfer coefficient data were initially obtained in liquid–solid fluidized beds both in the absence and presence of promoter and in homogeneous flow with promoter. In all these cases, the liquid-to-wall mass transfer coefficients were found to be in good agreement with those of Jagannadha Raju and Venkata Rao [8] and Sujatha et al. [9,10].

The measurement of individual phase holdups has been made using the methods described by Epstein [11]. The solids holdup,  $\varepsilon_s$  was determined from bed height measurements and the gas holdup,  $\varepsilon_g$  was determined from the pressure drop measurements. The liquid holdup,  $\varepsilon_L$  was thus obtained as  $1 - \varepsilon_s - \varepsilon_g$ . The equivalent diameter was obtained from the equation proposed by Ramesh et al. [12]. The axial velocities of liquid and gas were computed based on available flow area using the method described by Ramesh et al. [12]. The gas holdup thus obtained was found to be in good agreement with the equation of Soung [12,13].

**Table 1**  
Range of variables covered.

S. No.	Parameters studied	Minimum	Maximum	Max/min
1	Flow rate of gas ( $Q_g, \times 10^3$ ) (m <sup>3</sup> /s)	0	0.418	–
2	Flow rate of liquid ( $Q_L, \times 10^3$ ) (m <sup>3</sup> /s)	0.308	0.875	2.84
3	Diameters of the rod on which the tape is wound ( $d_r$ ) (cm)	1.27	1.90	1.49
4	Pitch of the promoter element ( $p$ ) (cm)	1.0	14.5	14.5
5	Width of the promoter element ( $w$ ) (cm)	0.3	1.2	4.00
6	Diameter of the particle ( $d_p$ ) (mm)	3.13	6.29	2.00
7	Bed porosity ( $\varepsilon$ )	0.486	0.973	2.00
8	Gas holdup ( $\varepsilon_g$ )	0	0.279	–
9	Liquid holdup ( $\varepsilon_L$ )	0.430	0.940	2.18
10	Solids holdup ( $\varepsilon_s$ )	0.027	0.514	17.92
11	Re	1065	18900	17.75
12	Re <sub>p</sub>	72.3	2087	28.86

### 3. Results and discussion

The axial velocities of both the liquid and gas are responsible for whatever dynamic changes that are occurring at the confining wall with regard to the boundary layer and its characteristics that control the diffusion of the reacting species to the wall or from the wall. The bed of solids, gas and promoter internal would occupy considerable volume of the test section obstructing the flow path for fluid electrolyte thus enhancing the dynamic behavior of the fluid electrolyte. The local velocities prevailing would significantly differ from the superficial velocity based on empty conduit cross-section.

#### 3.1. Effect of liquid and gas velocities

The present data on wall-to-bed mass transfer coefficient in three-phase fluidized beds in the absence of composite promoter corresponding to different constant gas velocities plotted against liquid velocity were shown in Fig. 2. These plots show that within the range of velocities covered in the present study, the liquid velocity has little effect and the coefficients were largely influenced by the gas velocity alone. Similar observations were reported by

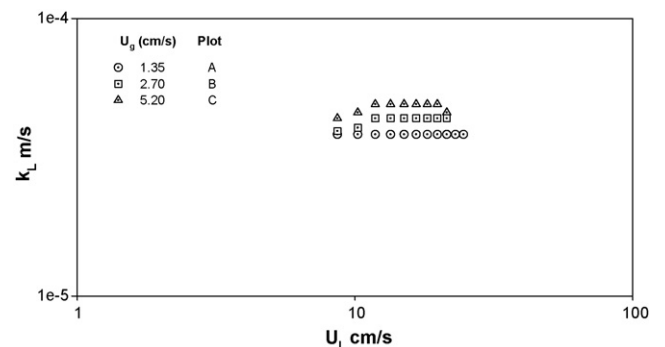


**Fig. 2.** Effect of gas velocity: variation of mass transfer coefficient with superficial liquid velocity in the absence of promoter for particle dia of 3.13 mm.

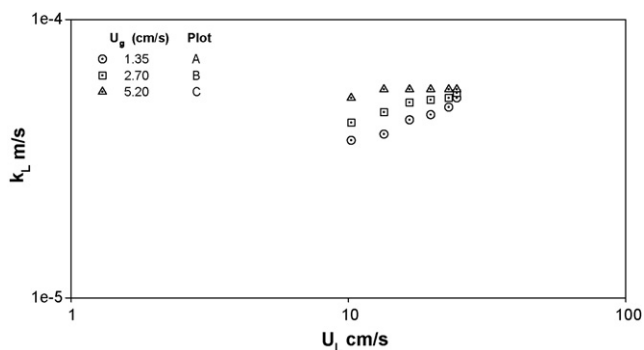


**Fig. 3.** Effect of gas velocity: variation of mass transfer coefficient with superficial liquid velocity in the presence of promotor {rod dia of 1.9 cm, tape pitch of 1.0 cm and tape width of 0.6 cm} for particle dia of 4.57 mm.

Ramesh et al. [4] in wall-to-bed mass transfer studies in annular flow.

Data on  $k_L$  in the presence of promotor internal ( $d_r = 1.9$  cm,  $p = 1.0$  cm and  $w = 0.6$  cm and for a particle size of 4.57 mm) were plotted against liquid velocity for three different gas velocities and shown in Fig. 3. At lower gas velocities ( $U_g < 5.2$  cm/s), the  $k_L$  was found to be a function of  $U_L$ . As the liquid velocity is increased, the coefficient approached a maximum equal to that at  $U_g = 5.2$  cm/s (Plot C). At higher gas velocities ( $U_g \geq 5.2$  cm/s) the data were found to be independent of liquid velocity.

### 3.2. Effect of particle diameter, $d_p$

The wall-to-bed mass transfer coefficient data obtained in a three-phase fluidized bed with a composite promotor as an internal ( $d_r = 1.9$  cm,  $p = 1.0$  cm and  $w = 0.9$  cm) were plotted against liquid velocity for a constant gas velocity ( $U_g = 2.7$  cm/s) for particles of three different sizes (viz., 3.13, 4.57 and 6.29 mm) and shown in Fig. 4. The plots revealed that the mass transfer coefficient increased upto 40% with a two-fold increase in particle diameter as shown in the inset (Fig. 4a) of the same figure. The fluidized bed condition with particles of 3.13 mm size has been approached relatively at lower velocities. The decline in the coefficients with particles of lower size ( $d_p = 3.13$  mm) indicating rear bed condition was conspicuous; the particles of higher size ( $d_p > 3.13$  mm) yielded higher coefficients and, further, they have shown a different trend; the coefficients obtained in this case remained nearly steady and constant over a wide range of liquid velocities (upto 25.0 cm/s) and no fall in the coefficients was noticed within the range of flow rates covered. The presence of composite promotor would have favored bubble disintegration to a more uniform size thus rendering the fluidized bed region more stable. The fluctuating behavior was found

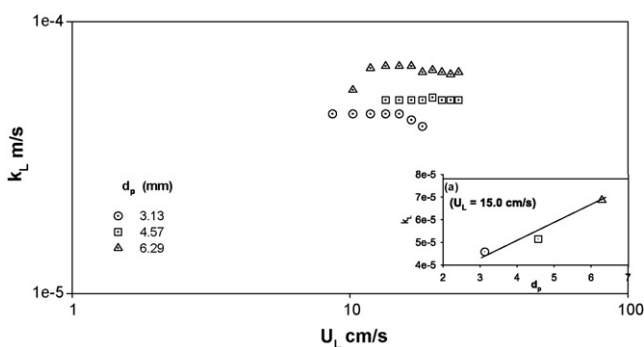


**Fig. 4.** Effect of particle diameter: variation of mass transfer coefficient with superficial liquid velocity in the presence of promotor {rod dia of 1.9 cm, tape pitch of 5 cm and tape width of 0.9 cm} at gas velocity  $U_g = 2.70$  cm/s.

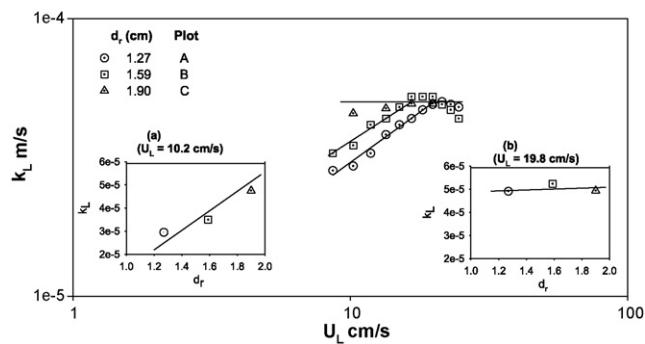


**Fig. 5.** Effect of promotor rod diameter: variation of mass transfer coefficient with superficial liquid velocity in the presence of promotor rods {tape pitch of 5 cm and tape width of 0.9 cm} at gas velocity  $U_g = 2.70$  cm/s for particle dia of 4.57 mm.

to be more pronounced in the absence of composite promotor in a three-phase fluidized bed, which may be attributed to continuous coalescing of the bubbles of random size.

### 3.3. Effect of central rod diameter, $d_r$

The effect of central rod diameter based on which the composite promotor was built was shown in Fig. 5 for three cases of central rod diameters, viz., 1.27, 1.59 and 1.9 cm. The helicoidal tape wound on these central rods has a pitch value of 5 cm and width of 0.9 cm. The parametric effect of rod diameter is conspicuous at lower liquid velocities. Plot C gives the maximum mass transfer coefficient data for  $d_r = 1.9$  cm, which was found to be independent of liquid velocity. The wall-to-bed mass transfer coefficient data corresponding to  $d_r$  values of 1.27 cm (Plot A) and 1.59 cm (Plot B), showed an increasing trend with increasing liquid velocity reaching a maximum  $k_L$  value, same as that obtained with a central rod of  $d_r = 1.9$  cm (Plot C). Beyond this, the wall-to-bed mass transfer coefficients remained steady and relatively constant. The  $k_L$  showed an increase with increase in rod diameter at lower liquid velocities (shown as a cross-plot in the inset (Fig. 5a) corresponding to a constant liquid velocity  $U_L = 10.2$  cm/s). At higher liquid velocities ( $U_L \geq 15$  cm/s), no noticeable effect was shown by the rod diameter as revealed through the inset (Fig. 5b) corresponding to a constant liquid velocity  $U_L = 19.8$  cm/s.

### 3.4. Effect of pitch and width

The pitch and width of the tape have shown a definite trend in case of the data in homogeneous flow. Sujatha et al. [9] reported that for a pitch value of 2.0 cm maximum value for  $k_L$  was obtained in a 5.0 cm i.d. test section. In a two-phase fluidized bed the earlier investigators [10] have not observed any noticeable effect of geometric variables of the composite promotor on the wall-to-bed mass transfer coefficient, in view of prevailing turbulence due to convective transport of the solids within the fluidized bed. The tape geometry  $w$  and  $p$  have not shown any effect on the  $k_L$  value and the promotor as a whole wielded some influence, may be due to a significant increase in the local velocity of the fluid electrolyte. Reduction in the cross-section of the flow geometry influenced the flow pattern at the reacting surface besides the severe scouring action of the fluidizing solids.

An attempt has been made to study the effect of the pitch of the composite promotor in a three-phase fluidized bed, in which the bubbling gas wielded considerable influence on the wall-to-bed mass transfer coefficients. Data on  $k_L$  were plotted and shown in Fig. 6, for the gas velocity 2.7 cm/s. The promotor with the geometry ( $d_r = 1.9$  cm,  $w = 0.6$  cm) but at varying pitches has been used as an internal. Although no definite trend with 'p' could be identified, the

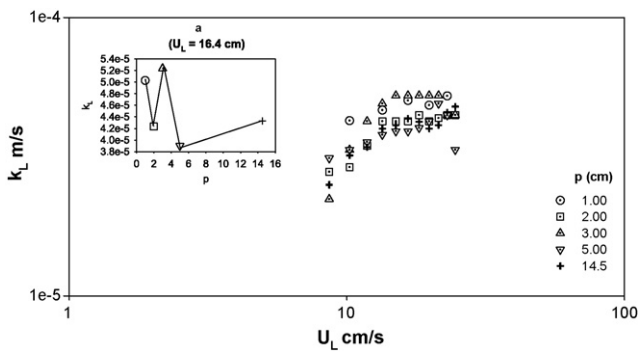


**Fig. 6.** Effect of tape pitch: variation of mass transfer coefficient with superficial liquid velocity at different tape pitches {rod dia of 1.9 cm and tape width of 0.6 cm} at gas velocity  $U_g = 2.70$  cm/s for particle dia of 4.57 mm.

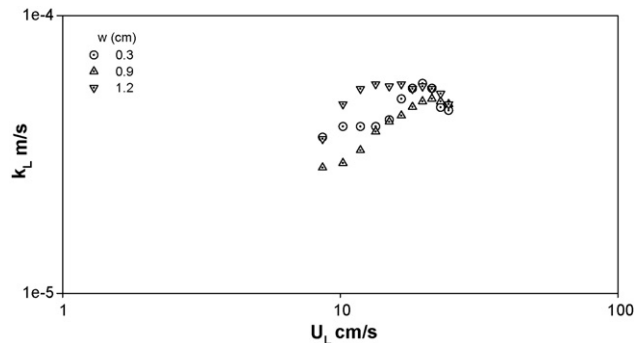


**Fig. 7.** Effect of tape width: variation of mass transfer coefficient with superficial liquid velocity at different tape widths {rod dia of 1.27 cm and tape pitch of 5 cm} at gas velocity  $U_g = 2.70$  cm/s for particle dia of 4.57 mm.

coefficients were found to be maximum for a pitch value of  $p = 3$  cm. Cross-plot (Fig. 6a) shown as in inset of Fig. 6 showed no definite trend in the pitch variation.

Plots of Fig. 7 show the effect of 'w' on mass transfer coefficient for a gas velocity of 2.7 cm/s. No systematic trend was found in the behavior of coefficients with width. At any value of 'w', the coefficients consistently increased with an increase in  $U_L$ . The increase with  $U_g$  however found to be marginal.

#### 4. Correlation

Data of the present study on the reduction of ferricyanide ion in three-phase fluidized beds with the composite promoter as internal were analyzed to arrive at the following  $j_D$ , Re format of equation. The entire data on reduction of ferricyanide ion, on regression yielded the following correlation equation:

$$j_D \varepsilon_L = 0.14 \left[ \left( \frac{Re_p \varepsilon}{\varepsilon_L (1 - \varepsilon)} \right) \left( 1 + \frac{p}{D_c} \right) \right]^{-0.23} \quad (2)$$

Average deviation: 7.5%  
Standard deviation: 9.9%

Eq. (2) equally represents the data in the absence of promoter in a three-phase fluidized bed. The data on oxidation of ferrocyanide ion are analyzed on the lines similar to those of reduction of ferricyanide ion. Eq. (2) could well represent the data on oxidation also within an average deviation of 10.3% and standard deviation of 12.5%. Fig. 8 shows the entire data on oxidation and reduction obtained in the present investigation plotted in accordance with Eq. (2).

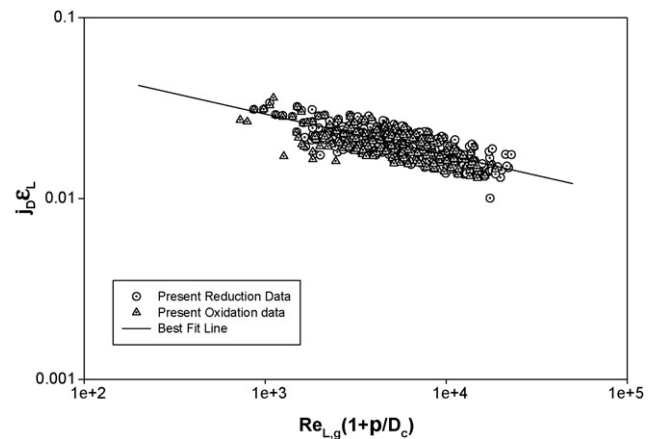


**Fig. 8.** Correlation plot of the data on both reduction and oxidation in accordance with Eq. (2).

#### 5. Conclusions

- Fluctuating bed behavior was found to be more pronounced in the absence of composite promoter.
- Effect of liquid velocity on wall-to-bed mass transfer coefficient is only marginal in the absence of promoter and mass transfer coefficients were largely influenced by gas velocities.
- The parametric effect of rod diameter is only seen at low liquid and gas velocities.
- No systematic trend in coefficients is observed with variations in pitch,  $p$  and width,  $w$  of the promoter geometry.
- Increase in particle diameter augmented the wall-to-bed mass transfer coefficients. In the range of particle diameters covered in the present study (3.13–6.29 mm) the augmentation was found to be upto a maximum of 40%.

#### References

- [1] S. Morooka, K. Kusakabe, Y. Kato, Mass transfer coefficient at the wall of a rectangular fluidized bed for liquid–solid and gas–liquid–solid systems, *Int. Chem. Eng.* 20 (1980) 433–438.
- [2] A. Yasunishi, M. Fukuma, K. Muroyama, Wall-to-liquid mass transfer in packed and fluidized beds with gas–liquid concurrent upflow, *J. Chem. Eng. Jpn.* 21 (1988) 522–528.
- [3] K.V. Ramesh, G.M.J. Raju, C. Bhaskara Sarma, R.V. Subba Raju, Liquid-wall mass transfer in three-phase fluidized beds with cross-flow of electrolyte, *Chem. Eng. J.* 135 (2008) 224–231.
- [4] K.V. Ramesh, G.M.J. Raju, C. Bhaskara Sarma, Ch.V.R. Murthy, R.V. Subba Raju, Liquid-wall mass transfer in three-phase fluidized beds with annular flow, *Indian Chem. Eng.* 50 (2008) 277–287.
- [5] K.V. Ramesh, Liquid-wall mass transfer in three-phase fluidized beds in the absence and presence of a composite promoter, PhD Thesis, Andhra University, Visakhapatnam, India (2006).
- [6] A.E. Bergles, Keynote at the 5th International Conference on Boiling Heat Transfer, Montego Bay, Jamaica, 4–8 May, 2003.
- [7] C.S. Lin, E.B. Denton, H.S. Gaskill, C.L. Putan, Diffusion controlled electrode reactions, *Ind. Eng. Chem.* 43 (1951) 2136–2143.
- [8] G.J.V. Jagannadha Raju, C. Venkata Rao, Ionic mass transfer in the presence of fluidizing solids, *Ind. J. Technol.* 3 (1965) 201–205.
- [9] V. Sujatha, C. Bhaskara Sarma, G.J.V. Jagannadha Raju, Studies on ionic mass transfer with coaxially placed helical tapes on a rod in forced convection flow, *Chem. Eng. Process.* 36 (1997) 67–73.
- [10] V. Sujatha, P. Rajendra Prasad, C. Bhaskara Sarma, G.J.V. Jagannadha Raju, Studies on ionic mass transfer with insert helical tape promoters in batch fluidized beds, *Indian J. Chem. Technol.* 10 (2003) 694–700.
- [11] N. Epstein, Three-phase fluidization: some knowledge gaps, *Can. J. Chem. Eng.* 59 (1981) 649–657.
- [12] K.V. Ramesh, G.M.J. Raju, G.V.S. Sarma, C. Bhaskara Sarma, Effect of internal on phase holdups of a three-phase fluidized bed, *Chem. Eng. J.* 145 (2009) 393–398.
- [13] W.Y. Soung, Bed expansion in three-phase fluidization, *Ind. Eng. Chem. Proc. Des. Dev.* 17 (1978) 33–36.